Wavelet Modeling of Contour Deformations in Sobolev Spaces for Fitting and Tracking Applications

Fernando Pérez Nava[a,*], Antonio Falcón Martel[b]

[a]Dep. de Estadística, Investigación Operativa y Computación. Universidad de La Laguna. Tenerife. Spain.
[b]Dep. de Informática y Sistemas. Universidad de Las Palmas de Gran Canaria. Gran Canaria. Spain.

Abstract. This paper proposes a new model for contour deformations using wavelets. This model uses Sobolev spaces to control the smoothness of the contour deformation. This formulation defines a probabilistic model that induces a prior distribution for contour deformation. Based on this distribution, the fitting problem is solved in bayesian terms. The deformation model is also used to generate a prior dynamic model for contour evolution in time. This probabilistic model is then applied to solve the tracking problem. Computational results for several real image problems are given for both the Kalman and Condensation filters.

Keywords: Active contours; Deformation modeling; Wavelets; Sobolev spaces; Contour fitting; Contour tracking; Kalman filter; Condensation Filter.

1 Introduction

Deformable models [1] are object models that possess shape-varying capability, which makes them suitable for representing non-rigid objects. A deformable model is usually described by a vector of parameters that span a multidimensional space. Usually deformations are confined in a region of the whole space and prior information about preferred deformations of the model can be obtained. This preference is then expressed in terms of a deformation energy (or cost) that penalizes some deformations. The importance of this prior information is that it simplifies and increases the robustness of the solutions to some problems like fitting and tracking. The deformation energy is coupled with a data mismatch criterion that measures the degree of discrepancy between the model and some measures extracted from an image. Model matching can then be formulated as an optimization problem of a combined criterion function that is defined in terms of both the deformation and the mismatch energy.

An important subset of deformable models is active contour models where an object is characterized by its external shape. They can be divided into parametric models and non-parametric models depending on the structure they assume about the object's shape. An example of non-parametric deformable model is the snake [2]. The deformation energy is a combination of forces controlling elasticity and stiffness and tends to produce smooth contours. The mismatch energy drives the model towards image features like image intensity or gradient magnitude. Snakes however have several problems that have been recognized: slow convergence because of the large number of coefficients to optimize or the lack of robustness of the fitting solution in noisy environments. To alleviate the limitations of non-parametric models, parametric representations have been proposed. An alternative approach to snakes, which also circumvents some of its problems, is to use a parametric b-spline representation of the curve, first introduced as b-snake [3]. Such formulation is characterized by less parameters and smoothness constraints built into the model. However, the snake deformation energy is too general and often it is not enough to obtain a stable behavior so more prior knowledge needs to be compiled in the model. This can

*Corresponding author: Tel: +34 – 922 - 319184; Fax: +34 – 922 -319202 E-mail: fdoperez@ull.es
This work has been partially supported by research project UE/DGS 1FD1997-1580-C02-02

be done restricting deformations to those generated from a predefined reference shape. Staib et al. [4] have used elliptic Fourier descriptors to represent contours that are smooth and continuously deformable. The parameters of the deformable contours are the Fourier coefficients. A probability distribution on the Fourier coefficients is specified so that there is a flexible bias towards some particular shape. The spread of the distribution is governed by the variability among instances of the object class. A bayesian decision rule is then used to obtain the optimal fitting of the boundary to the image, where the mismatch energy is based on the correlation between the contour and the boundary strength in the image. A similar approach is taken in [5] where shapes are represented in terms of b-splines. In this case, deformations from the reference shape are linearly parameterized obtaining linear shape spaces that can be related to geometric deformations. Restriction to linear parameterization has certain advantages in simplifying fitting algorithms and avoiding problems with local minima.

A natural extension of the fitting problem is the tracking problem, a topic of considerable interest in computer vision due to its applications [6], [7], [8]. In the tracking problem, the deformable model has to be fitted in every frame of a sequence so the requirements for robustness are of great importance. As we have seen in the fitting problem, one way to enforce robustness is to use prior information about shape deformations. In the dynamic case this is obtained from information about the dynamic evolution of the contour. The tracking problem becomes a two-phase problem in which the dynamic model is used for prediction from one discrete time to the next. Then the predicted contour is refined using the measures obtained from the image and these two phases are repeated again with the next frame from the sequence.

In this paper new prior models for both fitting and tracking problems are presented. These models are based on a wavelet representation of shape [9], [10], [11] and Sobolev smoothness spaces. There are a number of salient features in wavelet transforms that make wavelet-domain processing attractive [12]:

- Locality: Each wavelet coefficient represents the signal content localized in spatial location and frequency.

- Multiresolution: The wavelet transform analyses the signal at a nested set of scales with different resolutions.

- Energy Compaction: A wavelet coefficient is large only if singularities are present within the support of the wavelet basis. Therefore in contrast with other approaches, we need to model only a small number of coefficients. This is of great importance in real-time applications.

- Decorrelation: The wavelet transform of real world signals tend to be approximately decorrelated.

We will use the relation between wavelets and smoothness spaces to build wavelet contour representations with a desired degree of smoothness. In contrast with other approaches like snakes, different levels of smoothness can be defined and smooth deformations can be enforced without the necessity to alter the balance between the uncertainty of the prior model for deformations and data extracted from the image. This wavelet representation is also set in probabilistic terms so that the realizations of the stochastic model are almost sure in a predefined smoothness space. To solve the tracking problem we define wavelet-based dynamic models that establish a prior for possible motions. These dynamic models are also based in the smoothness results for the fitting problem. To increase the robustness of the approach these wavelet models are also expressed in terms of linear shape spaces and their properties are discussed. We also present experimental results for both the fitting and tracking problem in which the Kalman and Condensation filter have been employed.

This paper is divided in nine parts: in Section 2 a wavelet-based deformation model is presented and its relation with Sobolev spaces is established. In Section 3 we introduce the probabilistic deformation model and then in Section 4 we express the deformation models in terms of linear shape space. In Section 5 and 6 these results are combined to solve the fitting problem in bayesian terms. To study the tracking problem, in Section 7 wavelet based dynamic models are presented and these models are applied in Section 8. Finally in Section 9 we present the conclusions of this paper.

2 Wavelet-based deformation modeling in Sobolev spaces

Deformation models for wavelet representations of shape are related to functional smoothness spaces. In this paper, Sobolev spaces will be used in which the smoothness of the deformation can be parametrically specified. It will be shown how the smoothness of the contour is related to the coefficients of its representation by means of the contour norm in Sobolev space.

2.1 Wavelet Shape Representation

A wavelet basis uses translations and dilations of a scaling function f and a wavelet function y. If translations and dilations of both functions are orthogonal, a one dimensional function f can be expressed as [13], [14]:

$$f(u) = \sum_l c_{j_0,l} f_{j_0,l}(u) + \sum_{j \geq j_0,l} d_{j,l} y_{j,l}(u) \qquad j,l \in \mathrm{Z}, \tag{2.1}$$

where dilations and translations of scaling and wavelet functions are denoted by:

$$f_{j,l}(u) = 2^{j/2} f(2^j u - l), \quad j,l \in \mathrm{Z}, \qquad y_{j,l}(u) = 2^{j/2} y(2^j u - l), \quad j,l \in \mathrm{Z}, \tag{2.2}$$

and coefficients $c_{j,l}$ and $d_{j,l}$ in the function expansion are evaluated as:

$$c_{j_0,l} = \int_{-\infty}^{\infty} f(u) f_{j_0,l}(u) du, \qquad d_{j,l} = \int_{-\infty}^{\infty} f(u) y_{j,l}(u) du. \tag{2.3}$$

Let then $\boldsymbol{r}(u) = (x(u), y(u))$ be a parameterized closed planar curve that represents the shape of an object of interest. If the wavelet transform is applied independently to each of the $x(u)$, $y(u)$ functions, we can describe the planar curve in terms of a decomposition of $\boldsymbol{r}(u)$:

$$\boldsymbol{r}(u) = \sum_l \boldsymbol{c}_{j_0,l} f_{j_0,l}(u) + \sum_{j \geq j_0,l} \boldsymbol{d}_{j,l} y_{j,l}(u), \quad \boldsymbol{c}_{j_0,l} = (c_{j_0,l;x}, c_{j_0,l;y})^{\mathrm{T}}, \ \boldsymbol{d}_{j,l} = (d_{j,l;x}, d_{j,l;y})^{\mathrm{T}}, \tag{2.4}$$

where subindex x and y represent coordinate function pertenence and superscript T denotes the transpose operation. If the curve $\boldsymbol{r}(u)$ is closed and parameter u belong to an interval $I=[0,L]$ then we obtain the representation:

$$\boldsymbol{r}(u) = \boldsymbol{c}_{0,0} f_{0,0}(u) + \sum_{\substack{j \geq 0 \\ 0 \leq l < 2^j}} \boldsymbol{d}_{j,l} y_{j,l}(u), \tag{2.5}$$

with the coefficients in the curve expansion defined as:

$$\boldsymbol{c}_{0,0} = \Big(\big\langle x(u), f_{0,0}(u) \big\rangle, \big\langle y(u), f_{0,0}(u) \big\rangle\Big)^{\mathrm{T}}, \quad \boldsymbol{d}_{j,l} = \Big(\big\langle x(u), y_{j,l}(u) \big\rangle, \big\langle y(u), y_{j,l}(u) \big\rangle\Big)^{\mathrm{T}}, \tag{2.6}$$

where <,> denotes the scalar product:

$$\langle f, g \rangle = \frac{1}{L} \int_0^L f(u)\, g(u) du. \tag{2.7}$$

Basis and wavelet functions are normalized so that:

$$\| f_{0,0} \|_{L_2(I)} = \| y_{j,l} \|_{L_2(I)} = 1, \quad \text{with: } \| f \|^2_{L_2(I)} = \langle f, f \rangle. \tag{2.8}$$

In practice, we will work with finite number of coefficients in the representation:

$$\boldsymbol{r}(u) = \boldsymbol{c}_{0,0} f_{0,0}(u) + \sum_{\substack{0 \le j < J \\ 0 \le l < 2^j}} \boldsymbol{d}_{j,l} y_{j,l}(u), \tag{2.9}$$

obtaining a curve with $2N$ degrees of freedom ($N = 2^J$). Curve representation in terms of wavelets leads to a multiresolution decomposition of shape as seen on Figure 1.

Figure 1 about here

Curve expansion can be concisely written in matrix form. First we express scaling and wavelet functions in a vector as:

$$\boldsymbol{G}_W(u) = (f_{0,0}(u), \; y_{0,0}(u), \; \dots \; y_{J-1,2^{J-1}-1}(u))^{\mathrm{T}}, \tag{2.10}$$

then we can write coordinate functions as:

$$x(u) = \boldsymbol{G}_W(u)^{\mathrm{T}} \boldsymbol{w}^{\boldsymbol{x}}, \quad y(u) = \boldsymbol{G}_W(u)^{\mathrm{T}} \boldsymbol{w}^{y}, \tag{2.11}$$

with scaling and wavelet coefficients in vectors $\boldsymbol{w}^{\boldsymbol{x}}$ and $\boldsymbol{w}^{\boldsymbol{y}}$ defined as:

$$\boldsymbol{w}^{\boldsymbol{x}} = (c_{0,0;x}, \; d_{0,0;x}, \; \dots \; d_{J-1,2^{J-1}-1;x})^{\mathrm{T}}, \; \boldsymbol{w}^{y} = (c_{0,0;y}, \; d_{0,0;y}, \; \dots \; d_{J-1,2^{J-1}-1;y})^{\mathrm{T}}. \tag{2.12}$$

Then to describe curve $\boldsymbol{r}$(u) in matrix form we must define:

$$\boldsymbol{F}_W(u) = \boldsymbol{I}_2 \otimes \boldsymbol{G}_W(u)^{\mathrm{T}} = \begin{pmatrix} \boldsymbol{G}_W(u)^{\mathrm{T}} & \boldsymbol{0}_N^{\mathrm{T}} \\ \boldsymbol{0}_N^{\mathrm{T}} & \boldsymbol{G}_W(u)^{\mathrm{T}} \end{pmatrix}, \tag{2.13}$$

where $\otimes$ denotes the Kronecker product and $\mathbf{0}_N$ a null vector of N components. Note that due to the orthogonality of scaling and wavelet functions matrix $\boldsymbol{F}_W(u)$ verifies:

$$\frac{1}{L}\int_0^L \boldsymbol{F}_W(u)^{\mathrm{T}}\boldsymbol{F}_W(u)\,du = \boldsymbol{I}_{2N}\,, \tag{2.14}$$

where $\boldsymbol{I}_{2N}$ denotes the identity matrix of size $2N$

Also we define vector $\boldsymbol{w}$ as $\boldsymbol{w}=(\boldsymbol{w}^{x\,\mathrm{T}}, \boldsymbol{w}^{y\,\mathrm{T}})^{\mathrm{T}}$ and then we may write $\boldsymbol{r}(u)=\boldsymbol{F}_W(u)\boldsymbol{w}$. This matrix form will be used through the paper to describe $\boldsymbol{r}$.

2.2 Wavelet based Modeling of Curve Deformation

The theory of smoothness spaces [15] has an increasing importance in the field of signal and image processing. In order to control the smoothness of deformations we will consider Sobolev spaces $W^a(L_2(I))$, $0 < a < \infty$. These spaces have, very roughly speaking, "a derivatives in $L_2(I)$". Sobolev spaces are included in Besov spaces that are introduced as follows:

For $r > 0$ and $h > 0$, the r-th difference of a function f is defined as:

$$\Delta_h^{(r)} f(u) = \sum_{h=0}^{r}\binom{r}{k}(-1)^k f(u+kh), \quad u \in I_h^r = \{u \in I / u + rh \in I\}. \tag{2.15}$$

The $L_p(I)$-modulus of smoothness is defined as:

$$w_r(f,u)_p = \sup_{|h|\le u}\left\|\Delta_h^{(r)} f\right\|_{L_p(I_h^r)}, \tag{2.16}$$

then the Besov seminorm of index a is defined for $r > a$ by:

$$|f|_{B_q^a(L_p(I))} = \left(\int_0^\infty \left(\frac{w_r(f,u)_p}{t^a}\right)^q \frac{dt}{t}\right)^{1/q}, \tag{2.17}$$

finally the Besov space norm is then defined as:

$$\|f\|_{B_q^a(L_p(I))} = \|f\|_{L_p(I)} + |f|_{B_q^a(L_p(I))}. \tag{2.18}$$

The Besov space $B_q^a(L_p(I))$ is the class of functions in $L_p(I)$ satisfying $|f|_{B_q^a(L_p(I))} < \infty$.

Wavelets provide a simple characterization of Besov spaces [16]. Given a real function f defined over a compact subset I and analyzing scaling and wavelet functions f and y possessing $r > a$ vanishing moments, the Besov norm $\|f\|_{B_q^a(L_p(I))}$ is equivalent to the sequence norm:

$$\|f\|_{B_q^a(L_p(I))} \equiv |c_{0,0}| + \left(\sum_{j\geq 0} \left(\sum_{k=0}^{2^j-1} 2^{2aj} 2^{j(p/2-1)} |d_{j,k}|^p \right)^{q/p} \right)^{1/q}, \tag{2.19}$$

when $p = q = 2$ we obtain the Sobolev space $W^a(L_2(I))$. In this case we have:

$$\|f\|_{W^a(L_2(I))} \equiv |c_{0,0}| + \left(\sum_{j\geq 0} \sum_{k=0}^{2^j-1} 2^{2aj} |d_{j,k}|^2 \right)^{1/2}. \tag{2.20}$$

We propose to extend this characterization from real functions to contours. Then, given a contour $\boldsymbol{r}(u) = (x(u), y(u))$ for $r > 0$ and $h > 0$, the r-th difference of a contour $\boldsymbol{r}$ is extended to:

$$?_h^{(m)} \boldsymbol{r}(u) = \sum_{h=0}^{m} \binom{m}{k} (-1)^k \boldsymbol{r}(u + kh), \quad u \in I_h^r = \{u \in I / u + rh \in I\}. \tag{2.21}$$

The $L_2(I)$-modulus of smoothness is defined as:

$$w_m(\boldsymbol{r}, u)_2 = \sup_{|h|\leq u} \left\| ?_h^{(m)} \boldsymbol{r} \right\|_{L_2(I_h^r)}, \tag{2.22}$$

then the Sobolev seminorm of index a is defined for $m > a$ by:

$$|\boldsymbol{r}|_{W^a(L_2(I))} = \left(\int_0^\infty \left(\frac{w_m(\boldsymbol{r}, u)_2}{t^a} \right)^2 \frac{dt}{t} \right)^{1/2}, \tag{2.23}$$

finally the Sobolev space norm for curves is redefined as:

$$\|\boldsymbol{r}\|_{W^a(L_2(I))} = \|\boldsymbol{r}\|_{L_2(I)} + |\boldsymbol{r}|_{W^a(L_2(I))}, \text{ where:} \tag{2.24}$$

$$\|\boldsymbol{r}\|_{L_2(I)} = \left(\int_I \|\boldsymbol{r}\|^2 du \right)^{1/2} = \left(\int_I \left| \sqrt{x(u)^2 + y(u)^2} \right|^2 du \right)^{1/2}. \tag{2.25}$$

From the preceding definitions we obtain that for a curve $\mathbf{C} \equiv \boldsymbol{r}(u) = (x(u), y(u))^T$ the following norms are equivalent:

$$\|\boldsymbol{r}\|_{W^a(L_2(I))} \equiv \|x\|_{W^a(L_2(I))} + \|y\|_{W^a(L_2(I))}. \tag{2.26}$$

This result can be easily proved noting that two positive constants A, B can be found such that:

$$A(|x| + |y|) \leq \left(\sqrt{(|x|^2 + |y|^2)} \right) \leq B(|x| + |y|). \tag{2.27}$$

So the defined norm for curves is equivalent to the "natural" norm in $W^a(L_2(I))\times W^a(L_2(I))$. Therefore a curve belongs to the extension of $W^a(L_2(I))$ if and only if its coordinate functions belong to that space. The extension to curves of the Sobolev space also allows to express the norm in this space in terms of the coefficients of the curve expansion in wavelet basis as in (2.20):

Theorem 1

Let a curve $\mathbf{C} \equiv \boldsymbol{r}(u) = (x(u), y(u))^T$ be decomposed on its wavelet representation then its Sobolev norm $\|\boldsymbol{r}\|_{W^a(L_2(I))}$ is equivalent to the expression:

$$\|\boldsymbol{r}\|_{W^a(L_2(I))} \equiv \sqrt{\left|c_{0,0;x}\right|^2 + \left|c_{0,0;y}\right|^2} + \left(\sum_{j\geq 0}\sum_{k=0}^{2^j-1} 2^{2aj}\left(\left|d_{j,k;x}\right|^2 + \left|d_{j,k;y}\right|^2\right)\right)^{1/2}. \tag{2.28}$$

Proof is again based on inequality (2.27).

3 Wavelet probabilistic deformation model in Sobolev spaces.

The contour fitting and tracking problem can be formulated in probabilistic terms that allow an explicit representation for the uncertainty. In this section probabilistic models for contour deformation are derived and their properties are studied.

The simplest wavelet transform statistical models are obtained by assuming that the coefficients are independent. Under the independence assumption, modeling reduces to simply specifying the marginal distribution of each wavelet coefficient. The primary independent models employed to date are the generalized gaussian distribution (related to Besov spaces) and the gaussian mixture distribution. It can be shown that the gaussian distribution is related to Sobolev spaces by means of the following result [12]:

Theorem 2

Let $f(x)$ a real function where x is a real variable. Let it be decomposed in wavelet coefficients and suppose each coefficient is independently and identically distributed as:

$$d_{j,k} \sim N(0, s_j^2), \qquad s_j = 2^{-jb} s_0, \tag{3.1}$$

with $b > 0$ and $s_0 > 0$. Then the realizations of the probabilistic model are almost surely in the Sobolev Space $W^\alpha(L_2(I))$ if and only if $b > \alpha + 1/2$.

This result is extended to contours by the following theorem:

Theorem 3

Let a curve $\mathbf{C} \equiv \boldsymbol{r}(u) = (x(u), y(u))^T$ be decomposed on its wavelet representation and suppose that the vectors of its representation $\boldsymbol{d}_{j,k}$ are independently and identically distributed as:

$$\boldsymbol{d}_{j,k} = (d_{j,k;x}, d_{j,k;y})^T \sim N(\mathbf{0}_2, s_j^2 \boldsymbol{I}_2), \qquad s_j = 2^{-jb} s_0,\ b > 0 \text{ and } s_0 > 0, \tag{3.2}$$

then the realizations of the model are almost surely in the curve extension of the Sobolev Space $W^\alpha(L_2(I))$ if and only if $b > \alpha + 1/2$.

Theorem 3 can be proved from Theorem 2 noting that the probabilistic model in (3.2) implies that both coordinate functions are in $W^{\alpha}(L_2(I))$.
This result shows that the exponential decay of the variances $s_j=2^{-jb}s_0$ can be used to enforce the smoothness of the contours generated from the probabilistic model. In Figure 2 we can see an example of contours generated from the probabilistic model in (3.2) for several values of b. In discontinuous line we show the mean shape and in light grey we can see some random samples from the model. As expected, for greater values of b the contours generated are smoother.

Figure 2 about here

To complete the definition of the model we have to specify the distribution for the coefficient associated with the scaling function $\boldsymbol{c}_{0,0.}$ This coefficient (3.3) is associated with a translation of shape and we will assume that it is normally distributed and independent of the non-translation components $\boldsymbol{d}_{j,k.}$ This obviously does not change the pertenence of the curve to its Sobolev Space.

$$\boldsymbol{c}_{0,0} = \begin{pmatrix} c_{0,0,x} \\ c_{0,0,y} \end{pmatrix} \sim \boldsymbol{N}(\boldsymbol{0}_2, s_{TR}^2 \boldsymbol{I}_2). \tag{3.3}$$

We will use these distributions to model both deformations and changes of shape between frames. The wavelet probabilistic deformation model in (3.2) and (3.3) can be expressed in matrix form as:

$$\mathrm{P}(\boldsymbol{r}) \equiv \mathrm{P}(\boldsymbol{w}) \propto \exp\left(-\frac{1}{2}\boldsymbol{w}^{\mathrm{T}}\boldsymbol{S}_w\boldsymbol{w}\right), \quad \boldsymbol{r} = \boldsymbol{F}_W\boldsymbol{w}, \quad \text{with:} \tag{3.4}$$

$$\boldsymbol{S} = \boldsymbol{S}_w^{-1} = \boldsymbol{I}_2 \otimes \begin{pmatrix} s_{TR}^2 & 0 & \cdots & 0 \\ 0 & s_{DEF}^2 2^{-2b0} & \cdots & 0 \\ \vdots & \vdots & \cdots & \vdots \\ 0 & 0 & \cdots & s_{DEF}^2 2^{-2b(J-1)} \end{pmatrix}. \tag{3.5}$$

As shown before, parameter b is related to the smoothness of the deformation. It can be shown that parameters s_{TR}^2 and s_{DEF}^2 are related to the uncertainty of the contour. If a curve $\mathbf{C} \equiv \boldsymbol{r}(u) = (x(u), y(u))^{\mathrm{T}}$ is decomposed on its wavelet representation and its deformations are given by the wavelet probabilistic model shown in (3.4) and (3.5), then the mean square displacement $\bar{r}^2$ verifies:

$$\bar{r}^2 = \mathrm{Trace}(S). \tag{3.6}$$

This result, which is adapted from [17], allows the mean square displacement $\bar{r}^2$ to be decomposed in terms of the mean square displacement due to translation and non-translation $\bar{r}^2_{TR}$ and $\bar{r}^2_{DEF}$ as:

$$\bar{r}^2 = \bar{r}^2_{TR} + \bar{r}^2_{DEF}, \quad \bar{r}^2_{TR} = 2s^2_{TR}, \quad \bar{r}^2_{DEF} = 2s^2_{DEF}\frac{1-N^{-2b+1}}{1-2^{-2b+1}}, \; b > 1/2, \tag{3.7}$$

where N is the number of wavelet coefficients in the decomposition of the parametric functions as defined in (2.9). In the limiting case we have:

$$\lim_{N\to\infty} \bar{r}^2_{DEF} = 2s^2_{DEF}\frac{1}{1-2^{-2b+1}}, \; b > 1/2. \tag{3.8}$$

These formulas allow us to determine the parameters s^2_{TR} and s^2_{DEF} if we have an estimate of b and the uncertainty in displacement $\bar{r}^2_{TR}$ and $\bar{r}^2_{DEF}$.

4. Wavelet based deformation models in shape spaces

In certain applications it is possible to reduce the number of degrees of freedom in the model constraining its deformations. A linear shape-space $L(\boldsymbol{H}, \bar{\boldsymbol{w}})$ [18] is a linear mapping $\boldsymbol{w} = \boldsymbol{H}\boldsymbol{x} + \bar{\boldsymbol{w}}$ of a "shape space vector" $\boldsymbol{x} \in \mathrm{R}^{N_X}$ to a wavelet vector $\boldsymbol{w} \in \mathrm{R}^{N_W}$ where $\boldsymbol{H}$ is a $N_W \times N_X$ "shape matrix" that will be assumed of full rank. The vector $\bar{\boldsymbol{w}}$ represents a base curve against which shape variations are measured. Several shape spaces can be constructed: from geometric shape spaces like euclidean similarity and affine, to learned shape spaces derived from the PCA transform. Below we show the derivation of some geometric shape spaces:

a) Euclidean similarity shape space

The similarity space for a base curve $\bar{\boldsymbol{r}}$ with parameter vector $\bar{\boldsymbol{w}}$ form a 4-dimensional shape space with shape matrix:

$$\boldsymbol{H} = \begin{pmatrix} \boldsymbol{T} & \boldsymbol{0}_N & \bar{\boldsymbol{w}}^x & -\bar{\boldsymbol{w}}^y \\ \boldsymbol{0}_N & \boldsymbol{T} & \bar{\boldsymbol{w}}^y & \bar{\boldsymbol{w}}^x \end{pmatrix}, \quad \boldsymbol{T} = (1, \boldsymbol{0}^{\mathrm{T}}_{N-1})^{\mathrm{T}}. \tag{4.1}$$

Without loss of generality we will assume that the curve has its centroid on the origin so that the first two columns are orthogonal to the rest. This makes these columns to be associated with translations while the rest are associated with dilation and rotation.
With this definition for the shape matrix, shape space vector $\boldsymbol{x}=(a, b, k\,(\cos(q)-1), k\,(\sin(q)))$, translates the curve determinated by $\bar{\boldsymbol{w}}$ a units on the x-axis and b units on the y-axis, obtaining also a rotation with angle q and a scaling with factor k.

b) Planar affine shape space

The affine space for a base curve $\bar{\boldsymbol{r}}$ with parameter vector $\bar{\boldsymbol{w}}$ form a 6-dimensional shape space and represents the set of affine transformations $\boldsymbol{r}=\boldsymbol{t}+\boldsymbol{M}\bar{\boldsymbol{r}}$ that can be applied to that curve, where $\boldsymbol{t}$ is a bidimensional translation vector and $\boldsymbol{M}=(m_{ij})$ is a square matrix of order two. In this case the shape matrix is defined as:

$$\boldsymbol{H} = \begin{pmatrix} \boldsymbol{T} & \boldsymbol{0}_N & \overline{\boldsymbol{w}}^x & \boldsymbol{0}_N & \boldsymbol{0}_N & \overline{\boldsymbol{w}}^y \\ \boldsymbol{0}_N & \boldsymbol{T} & \boldsymbol{0}_N & \overline{\boldsymbol{w}}^y & \overline{\boldsymbol{w}}^x & \boldsymbol{0}_N \end{pmatrix}, \quad \boldsymbol{T} = (1, \boldsymbol{0}_{N-1}^{\mathrm{T}}). \tag{4.2}$$

Without loss of generality we will assume again that the curve has its centroid on the origin so that the first two columns are orthogonal to the rest. Then shape space vector $\boldsymbol{x}=(a, b, m_{11}-1, m_{22}-1, m_{21}, m_{12})$, displaces the curve determinated by $\overline{\boldsymbol{w}}$ a units on the x-axis and b units on the y-axis obtaining also a transformation of the curve with matrix $\boldsymbol{M}=(m_{ij})$.

c) Key frames shape space

Another way to construct a shape space is to use some representative outlines of the object's shape. Often, an effective shape space can be built by linear combination of these frames. For example, given a base curve $\overline{\boldsymbol{r}}$ with parameter vector $\overline{\boldsymbol{w}}$ and a key frame $\boldsymbol{w}_k$ we can form a 6-dimensional shape space combining their euclidean similarities by means of shape matrix:

$$\boldsymbol{H} = \begin{pmatrix} \boldsymbol{T} & \boldsymbol{0}_N & \overline{\boldsymbol{w}}^x & -\overline{\boldsymbol{w}}^y & \boldsymbol{w}_1^x & -\boldsymbol{w}_1^y \\ \boldsymbol{0}_N & \boldsymbol{T} & \overline{\boldsymbol{w}}^y & \overline{\boldsymbol{w}}^x & \boldsymbol{w}_1^y & \boldsymbol{w}_1^x \end{pmatrix}, \quad \boldsymbol{T} = (1, \boldsymbol{0}_{N-1}^{\mathrm{T}})^{\mathrm{T}}, \quad \boldsymbol{w}_1 = \boldsymbol{w}_k - \overline{\boldsymbol{w}}. \tag{4.3}$$

With this definition for the shape matrix, we obtain $\boldsymbol{w}_k$ with shape space vector $\boldsymbol{x}$ = (0, 0, 0, 0, 1, 0).

5 Probabilistic models in shape space

The probabilistic model defined in Section 3 for wavelet space induces a probabilistic model in shape space:

$$\mathrm{P}(\boldsymbol{x}) \propto \exp\left(-\frac{1}{2}\boldsymbol{x}^T \boldsymbol{S}_{\boldsymbol{x}}\ \boldsymbol{x}\right), \quad \boldsymbol{S}_{\boldsymbol{x}} = \boldsymbol{H}^{\mathrm{T}} \boldsymbol{S}_w \boldsymbol{H}, \tag{5.1}$$

where $\boldsymbol{S}_w$ is defined in (3.5).
Both probabilistic models are related since probabilistic distribution in $\boldsymbol{x}$ generates the deformations that result from the oblique projection of the deformed contours in wavelet space over the shape space. Formally, if $\boldsymbol{x}$ is a random shape variable with distribution $\boldsymbol{x} \sim \boldsymbol{N}(\boldsymbol{0}_{N_x}, \boldsymbol{S}_{\boldsymbol{x}}^{-1})$ and $\boldsymbol{w}$ is a random wavelet variable with distribution $\boldsymbol{w} \sim \boldsymbol{N}(\overline{\boldsymbol{w}}, \boldsymbol{S}_{\boldsymbol{w}}^{-1})$, suppose that shape space $L(\boldsymbol{H}, \overline{\boldsymbol{w}})$ is expressed as $\boldsymbol{w} = \boldsymbol{H}\boldsymbol{x} + \overline{\boldsymbol{w}}$, then if we define the weighted pseudoinverse $\boldsymbol{H}_{\boldsymbol{S}_w}^{+}$ and the oblique projection matrix $\boldsymbol{P}_{\boldsymbol{S}_w}$ as:

$$\boldsymbol{H}_{\boldsymbol{S}_w}^{+} = (\boldsymbol{H}^{\mathrm{T}} \boldsymbol{S}_w \boldsymbol{H})^{-1} \boldsymbol{H}^{\mathrm{T}} \boldsymbol{S}_w, \quad \boldsymbol{P}_{\boldsymbol{S}_w} = \boldsymbol{H}\boldsymbol{H}_{\boldsymbol{S}_w}^{+}, \tag{5.2}$$

then $\boldsymbol{H}\boldsymbol{x} + \overline{\boldsymbol{w}}$ and $\overline{\boldsymbol{w}} + \boldsymbol{P}_{\boldsymbol{S}_w}(\boldsymbol{w} - \overline{\boldsymbol{w}})$ share the same distribution.

As shown in (3.6) mean square displacement is related to the trace of the covariance matrix. Then if a curve $\mathbf{C} \equiv \boldsymbol{r}(u) = (x(u), y(u))^{\mathrm{T}}$ is decomposed on its wavelet representation and its deformations are given by $\boldsymbol{H}\boldsymbol{x} + \overline{\boldsymbol{w}}$ with $\boldsymbol{x} \sim \boldsymbol{N}(\boldsymbol{0}_{N_x}, \boldsymbol{S}_{\boldsymbol{x}}^{-1})$. Then the mean square displacement $\overline{r}^2$ around the contour can be expressed as:

$$\overline{r}^2 = \mathrm{Trace}(\boldsymbol{P}_{\boldsymbol{S}_w} \boldsymbol{S}). \tag{5.3}$$

Sometimes it may be desirable that the prior term influences the shape of the curve but not its position or orientation. To achieve the desired invariance over a subspace S_{INV} with oblique projection matrix $\boldsymbol{P}_{\boldsymbol{S}_w}^{INV}$ contained in shape space, the information matrix $\boldsymbol{S}_x$ in (5.1) is set to:

$$\boldsymbol{S}_{INV_x^-} = \boldsymbol{G}_{INV^-}^{\mathrm{T}} \boldsymbol{S}_x \boldsymbol{G}_{INV^-}, \tag{5.4}$$

through matrix $\boldsymbol{G}_{INV^-}$ that projects $\boldsymbol{x}$ in the complement S_{INV^-} of subspace S_{INV} by means of projection matrix $\boldsymbol{P}_{\boldsymbol{S}_w}^{INV^-}$, defined as:

$$\boldsymbol{G}_{INV^-} = \boldsymbol{H}_{\boldsymbol{S}_w}^{+} \boldsymbol{P}_{\boldsymbol{S}_w}^{INV^-} \boldsymbol{H}, \quad \boldsymbol{P}_{\boldsymbol{S}_w}^{INV^-} = (\boldsymbol{I}_{2N} - \boldsymbol{P}_{\boldsymbol{S}_w}^{INV}). \tag{5.5}$$

As an example, consider the affine shape space of a curve centered on its centroid and define the translation subspace as the invariant subspace. Then $\boldsymbol{G}_{INV^-}$ and $\boldsymbol{P}_{\boldsymbol{S}_w}^{INV^-}$ are defined as:

$$\boldsymbol{G}^{INV^-} = \begin{pmatrix} \boldsymbol{0}_{2\times 2} & \boldsymbol{0}_{2\times 4} \\ \boldsymbol{0}_{4\times 2} & \boldsymbol{I}_4 \end{pmatrix}, \quad \boldsymbol{P}_{\boldsymbol{S}_w}^{INV} = \boldsymbol{I}_2 \otimes \begin{pmatrix} 1 & \boldsymbol{0}_{N-1}^{\mathrm{T}} \\ \boldsymbol{0}_{N-1} & \boldsymbol{0}_{N-1\times N-1} \end{pmatrix} \tag{5.6}$$

This means that the last four components of the shape vector $\boldsymbol{x}$ account for the non-translational variation of shape.

2.3 Parameter Estimation

To complete the prior distribution it is necessary to provide values for the parameters in matrix S. These are related to the positional uncertainty of the contour and its smoothness. We will assume that the positional uncertainty parameters are known and try to estimate the smoothness parameter. Then, to obtain an estimator we solve the maximum likelihood equations that lead to:

$$\sum_{j=0}^{\log_2(N)-1} 2^{(2b+1)j} v_j^2 \, k_j = 0, \quad k_j = \left(\frac{1}{N-1} - \frac{j}{N(\log_2(N)-2)+2} \right) \text{with } v_j^2 = \sum_{l=0}^{2^j-1} d_{j,l,x}^2 + d_{j,l,y}^2 . \tag{5.7}$$

that is, a polynomial equation in $z=2^{2b+1}$.

6. The fitting problem

When the fitting problem is set in a probabilistic terms [17] we combine the prior density in shape space:

$$\mathrm{P}(\boldsymbol{x} \mid \bar{\boldsymbol{x}}) \propto \exp\left(-\frac{1}{2} (\boldsymbol{x} - \bar{\boldsymbol{x}})^{\mathrm{T}} \bar{\boldsymbol{S}} \, (\boldsymbol{x} - \bar{\boldsymbol{x}}) \right), \tag{6.1}$$

with the density function for the mismatch to the data that will be defined as:

$$\mathrm{P}(\boldsymbol{r}_D \mid \boldsymbol{r}) \equiv \mathrm{P}(\boldsymbol{w}_D \mid \boldsymbol{w}) \equiv \mathrm{P}(\boldsymbol{x}_D \mid x) \propto \exp\left(-\frac{1}{2} (\boldsymbol{x} - \boldsymbol{x}_D)^T \boldsymbol{S}_D \, (\boldsymbol{x} - \boldsymbol{x}_D) \right), \tag{6.2}$$

with information matrix:

$$\boldsymbol{S}_D = \frac{1}{s_D^2} \boldsymbol{H}^T \boldsymbol{H}, \tag{6.3}$$

and where wavelet and shape spaces are related by :

$$\boldsymbol{r}_D = \boldsymbol{F}_W \boldsymbol{w}_D, \quad \boldsymbol{w}_D = \boldsymbol{H}\boldsymbol{x}_D + \overline{\boldsymbol{w}}. \tag{6.4}$$

In this case the mean square displacement of the probabilistic model is given by:

$$\bar{r}^2 = N_X \, s_D^2 . \tag{6.5}$$

Now that the prior and adjustment probability density functions have been defined, to solve the fitting problem in bayesian terms we will evaluate the maximum a posteriori estimator:

$$\hat{\boldsymbol{x}} = \bar{\boldsymbol{x}} + \left(\boldsymbol{S}_D + \bar{\boldsymbol{S}} \right)^{-1} \boldsymbol{Z}, \quad \boldsymbol{Z} = \boldsymbol{S}_D \boldsymbol{x}_D, \quad \boldsymbol{x}_D = \boldsymbol{H}^+ (\boldsymbol{w}_D - \overline{\boldsymbol{w}}). \tag{6.6}$$

The covariance matrix gives the uncertainty of the fitting solution:

$$\hat{\boldsymbol{S}} = \left(\boldsymbol{S}_D + \bar{\boldsymbol{S}} \right)^{-1}. \tag{6.7}$$

In practice, we will only get a finite number of measurements along the curve $\boldsymbol{r}_D$ so we will get:

$$\mathrm{P}(\boldsymbol{r}_D \mid \boldsymbol{r}) \propto \exp\left(-\frac{1}{2s_D^2} \left\| \boldsymbol{r} - \boldsymbol{r}_D \right\|_{L_2(I)}^2 \right) \approx \exp\left(-\frac{1}{2s_D^2} \frac{1}{M} \sum_{i=1}^{M} \left| d\boldsymbol{r}(u_i) - \boldsymbol{F}_W(u_i) \boldsymbol{H} \, d\boldsymbol{x} \right|^2 \right), \tag{6.8}$$
$$d\boldsymbol{x} = (\boldsymbol{x} - \bar{\boldsymbol{x}}), \quad d\boldsymbol{r}(u_i) = (\boldsymbol{r}_D - \bar{\boldsymbol{r}})(u_i),$$

that can be written in matrix form as:

$$\exp\left(-\frac{1}{2s_D^2} \frac{1}{M} (\boldsymbol{D} - \boldsymbol{F}\boldsymbol{H}d\boldsymbol{x})^{\mathrm{T}} (\boldsymbol{D} - \boldsymbol{F}\boldsymbol{H}d\boldsymbol{x}) \right), \tag{6.9}$$
$$\boldsymbol{D} = (d\boldsymbol{r}(u_1)^{\mathrm{T}}, \cdots, d\boldsymbol{r}(u_M)^{\mathrm{T}})^{\mathrm{T}}, \quad \boldsymbol{F} = (\boldsymbol{F}_W(u_1)^{\mathrm{T}}, \ldots, \boldsymbol{F}_W(u_M)^{\mathrm{T}})^{\mathrm{T}},$$

then defining:

$$\boldsymbol{S}_D = \frac{1}{s_D^2} \frac{1}{M} (\boldsymbol{F}\boldsymbol{H})^{\mathrm{T}} \boldsymbol{F}\boldsymbol{H}, \tag{6.10}$$

we obtain the optimal solution:

$$\hat{\boldsymbol{x}} = \left(\overline{\boldsymbol{S}} + \boldsymbol{S}_D\right)^{-1} \boldsymbol{Z}, \quad \boldsymbol{Z} = \boldsymbol{S}_D \boldsymbol{D}. \tag{6.11}$$

Matrix calculations can be simplified to:

$$(\boldsymbol{FH})^{\mathrm{T}}(\boldsymbol{FH}) = \sum_{i=1}^{M} \boldsymbol{V}(u_i)\boldsymbol{V}(u_i)^{\mathrm{T}}, \quad (\boldsymbol{FH})^{\mathrm{T}} \boldsymbol{D} = \sum_{i=1}^{M} \boldsymbol{V}(u_i) d\boldsymbol{r}(u_i) \quad \text{with } \boldsymbol{V}(u_i) = (\boldsymbol{F}_W(u_i)\boldsymbol{H})^{\mathrm{T}}. \tag{6.12}$$

In Figure 3 we show a fitting example where we have a mouse on a laboratory cell. In this case the prior for the contour is the ellipse shown in light grey around the mouse and the final position for the contour is show on black. For each point in the initial contour we look for a corresponding point on the image searching along for the nearest border in the normal direction. We can see that this search will produce a false matching by the presence of the tail of the mouse. When no information about smoothness ($b = 0$) is provided this false matching generates a protrusion on the fitting solution introducing errors as can be seen in the image on the left. However, when we introduce as prior information that the deformation must be smooth ($b = 2.5$) the protrusion disappears as can be seen in the image of the right despite the false matching remains. Notice that in contrast with other approaches like snakes we do not weight more the prior term to enforce smoothness. Balance of uncertainties between prior and data measured by their mean square displacement $\overline{r}^2$ remains constant in both images, adjusting s_{DEF}^2 for the change is parameter b. This shows the importance of smoothness information to increase the robustness of the fitting process.

Figure 3 about here

7 Wavelet-based dynamic models in Sobolev spaces

In this section we present dynamic models for wavelets that define contour evolution in time to obtain a wavelet based solution of the tracking problem. The prior model presented for the fitting problem has to be extended to deal with the problem of tracking the curve over a sequence of images. Therefore it is necessary to provide not only a prior for the first frame but also a prior for possible motions. It must have a deterministic part, giving the expected displacement between frames and a stochastic part to measure the uncertainty about the predictions of the model.

In order describe shape motion a second order autoregressive AR(2) process will be used:

$$\boldsymbol{w}_t - \overline{\boldsymbol{w}} = \boldsymbol{A}_1 (\boldsymbol{w}_{t-1} - \overline{\boldsymbol{w}}) + \boldsymbol{A}_2 (\boldsymbol{w}_{t-2} - \overline{\boldsymbol{w}}) + \boldsymbol{B}\boldsymbol{n}_t, \tag{7.1}$$

where $\boldsymbol{A}_1$, $\boldsymbol{A}_2$, $\boldsymbol{B}$, are square matrices of order N_W and $\boldsymbol{n}_t$ is a vector normally distributed of mean $\boldsymbol{0}_{N_W}$ and covariance matrix equal to the identity. Therefore motion is decomposed as a deterministic drift plus a diffusion process that will be assured to be in the Sobolev space using the results in the preceding section.
The wavelet model leads to the model in shape space:

$$\boldsymbol{x}_t - \bar{\boldsymbol{x}} = \boldsymbol{A}_1 (\boldsymbol{x}_{t-1} - \bar{\boldsymbol{x}}) + \boldsymbol{A}_2 (\boldsymbol{x}_{t-2} - \bar{\boldsymbol{x}}) + \boldsymbol{B}\boldsymbol{n}_t, \tag{7.2}$$

where now $\boldsymbol{A}_1$, $\boldsymbol{A}_2$, $\boldsymbol{B}$, are square matrices of order N_X and $\boldsymbol{n}_t$ is a vector normally distributed of mean $\boldsymbol{0}_{N_X}$ and covariance matrix equal to the identity.

7.1 Harmonic motion in shape space

An interesting way to construct a dynamic model is to impose harmonic motion in shape space [17]. Then we have to choose:

$$\boldsymbol{A}_2 = a_2 \boldsymbol{I}, \quad \boldsymbol{A}_1 = a_1 \boldsymbol{I}, \quad \boldsymbol{B} = b\boldsymbol{S}_{\boldsymbol{x}}^{-1/2}, \tag{7.3}$$

with:

$$a_2 = -\exp(-2\,d\,t),\ a_1 = 2\exp(-d\,t)\cos(2\pi f\,t). \tag{7.4}$$

Parameter t represents the sample interval, d represents the damping rate and f the frequency of oscillation. In this case defining:

$$a^2 = \frac{(1-a_2)}{(1+a_2)(1-a_1-a_2)(1+a_1-a_2)}, \tag{7.5}$$

the steady state mean $\boldsymbol{E}_\infty$ and covariance matrix $\boldsymbol{C}_\infty$ verifies:

$$\boldsymbol{E}_\infty = \bar{\boldsymbol{x}}, \quad \boldsymbol{C}_\infty = b^2 a^2 \boldsymbol{S}_{\boldsymbol{x}}^{-1}, \tag{7.6}$$

then we can to obtain a mean square displacement $\bar{r}^2$ setting b to:

$$b = \frac{\bar{r}}{a\sqrt{\mathrm{Trace}(\boldsymbol{P}_{\boldsymbol{S}_w}\boldsymbol{S})}}. \tag{7.7}$$

7.2 Partitioned harmonic motion between subspaces

If we have a several orthogonal subspaces S_i with associated matrix in shape space $\boldsymbol{G}_i$ defined as in (5.5) motion can be decomposed in each subspace defining:

$$\boldsymbol{A}_1 = \sum_i a_{1,i}\boldsymbol{G}_i, \quad \boldsymbol{A}_2 = \sum_i a_{2,i}\boldsymbol{G}_i, \qquad \boldsymbol{B} = \sum_i b_i \boldsymbol{G}_i \boldsymbol{S}_x^{1/2}, \quad a_{1,i}, a_{2,i}, b_i \in \mathrm{R}. \tag{7.8}$$

This allows contour motion to be expressed decomposed on each subspace. If we define:

$$a_i^2 = \frac{(1-a_{2,i})}{(1+a_{2,i})(1-a_{1,i}-a_{2,i})(1+a_{1,i}-a_{2,i})}, \tag{7.9}$$

then the mean vector $\boldsymbol{E}_{\infty i}$ and covariance matrix $\boldsymbol{C}_{\infty i}$ for the limit distribution of the autoregressive model in subspace S_i verifies:

$$\boldsymbol{E}_{\infty i} = \boldsymbol{G}_i \bar{\boldsymbol{x}}, \quad \boldsymbol{C}_{\infty i} = b_i^2 a_i^2 \boldsymbol{G}_i \boldsymbol{S}_x^{-1} \boldsymbol{G}_i^{\mathrm{T}}, \tag{7.10}$$

and the total mean square displacement $\bar{r}^2$ can be obtained from the mean square displacement of each model $\bar{r}_i^2$ as: $\bar{r}^2 = \sum_i \bar{r}_i^2$.

As in (7.7) to obtain a mean displacement $\bar{r}_i$ we must set b_i to:

$$b_i = \frac{\bar{r}_i}{a_i \sqrt{\mathrm{Trace}(\boldsymbol{P}_{\boldsymbol{S}_w}^i \boldsymbol{S})}}, \tag{7.11}$$

then parameters related to the stochastic part of the model can be defined in terms of the deterministic parameters.

7.3 Constant velocity model

A subclass of harmonic motion is the constant velocity model in which $d = f = 0$. In this case there is no steady state and $\bar{r}_i^2$ cannot be used to characterize the stochastic component. Then it can be shown that the mean square displacement $\bar{r}^2(t)$ grows asymptotically:

$$\bar{r}(t) \approx g \; t^{3/2}, \quad b = \frac{g}{\sqrt{\mathrm{Trace}(\boldsymbol{P}_{\boldsymbol{S}_w} \boldsymbol{S})/3}} t^{3/2}. \tag{7.12}$$

8 The tracking problem.

In this section the results obtained from the wavelet based dynamical models are used in the contour tracking problem. The use of a gaussian density for the dynamic evolution and adjustment models in (6.2) and (7.2) poses the problem into the Kalman filter framework [19]. However this model is only valid in images of low complexity and clutter. In that case other approaches such as the Condensation [20] filter can be used to solve the tracking problem on more difficult domains.

8.1 Contour tracking with the Kalman filter

The Kalman filter is the natural mechanism for temporal fusion when the distributions are gaussian. It computes the evolution of the gaussian density for the state of the tracked object. Therefore it is only necessary to make explicit the equations for the time evolution for the mean and covariance matrix that defines the gaussian distribution.

The equations for the time evolution are divided on three steps [17]:

1. - Prediction

$$\hat{\boldsymbol{x}}_t^- = \overline{\boldsymbol{x}} + \boldsymbol{A}_1 (\hat{\boldsymbol{x}}_{t-1}^- - \overline{\boldsymbol{x}}) + \boldsymbol{A}_2 (\hat{\boldsymbol{x}}_{t-2}^- - \overline{\boldsymbol{x}}) , \ \hat{\boldsymbol{x}}_{t-1}^- = \hat{\boldsymbol{x}}_{t-1} , \tag{8.1}$$

$$\boldsymbol{R}_t'' = \boldsymbol{S}_{t-1}, \quad \boldsymbol{R}_t' = \boldsymbol{A}_2 \boldsymbol{S}_{t-1}'^{\mathrm{T}} + \boldsymbol{A}_1 \boldsymbol{S}_{t-1}, \quad \boldsymbol{R}_t = \boldsymbol{A}_2 \boldsymbol{S}_{t-1}'' \boldsymbol{A}_2^{\mathrm{T}} + \boldsymbol{A}_1 \boldsymbol{S}_{t-1}' \boldsymbol{A}_2^{\mathrm{T}} + \boldsymbol{A}_2 \boldsymbol{S}_{t-1}'^{\mathrm{T}} \boldsymbol{A}_1^{\mathrm{T}} + \boldsymbol{A}_1 \boldsymbol{S}_{t-1} \boldsymbol{A}_1^{\mathrm{T}} + \boldsymbol{B}_0 \boldsymbol{B}_0^{\mathrm{T}} . \tag{8.2}$$

2. - Measurement

Apply the fitting algorithm in Section 6 to the image at time t using $\hat{\boldsymbol{x}}_t^-$ as the mean value. Use $\boldsymbol{R}_t$ as the covariance matrix and obtain vector $\boldsymbol{Z}_t$ and matrix $\boldsymbol{S}_t$.

3. - Assimilation

$$\boldsymbol{K}_t' = \boldsymbol{R}_t' \left(\boldsymbol{I} + \boldsymbol{S}_t \boldsymbol{R}_t \right)^{-1}, \quad \boldsymbol{K}_t = \boldsymbol{R}_t \left(\boldsymbol{I} + \boldsymbol{S}_t \boldsymbol{R}_t \right)^{-1}, \tag{8.3}$$

$$\boldsymbol{S}_t'' = \boldsymbol{R}_t'' - \boldsymbol{K}_t' \boldsymbol{S}_t \boldsymbol{R}_t', \quad \boldsymbol{S}_t' = \boldsymbol{R}_t' - \boldsymbol{K}_t \boldsymbol{S}_t \boldsymbol{R}_t', \quad \boldsymbol{S}_t = \boldsymbol{R}_t - \boldsymbol{K}_t \boldsymbol{S}_t \boldsymbol{R}_t , \tag{8.4}$$

$$\hat{\boldsymbol{x}}_{t-1} = \hat{\boldsymbol{x}}_{t-1}^- + \boldsymbol{K}_t' \boldsymbol{Z}_t , \quad \hat{\boldsymbol{x}}_t = \hat{\boldsymbol{x}}_t^- + \boldsymbol{K}_t \boldsymbol{Z}_t . \tag{8.5}$$

Now we show an example of tracking with the Kalman filter. The problem to be solved is to follow the outline of a mouse in a laboratory cell. In this case the Kalman filter is appropriate since we are in a controlled and clutter free environment. However there are sources that may distract the tracker like the tail of the mouse and its reflections on the walls of the cell.

Change of position and deformation of the mouse is modeled from three components. The first component is a translation movement. The second component is an elongation that is modeled through a key frame (see Section 4). The third component is a smooth deformation on the complement subspace. The mouse has a vivid movement on the translational and key frame subspaces and a moderate movement on the complement subspace. The dynamic model used is the partitioned harmonic motion between subspaces. In this example the parameters shown in (7.4) and (7.12) that define the dynamic model have been fixed in each subspace (7.8) to:

Table 1 about here

The election of the parameters show the constant velocity model on the translation subspace. In the key frame subspace we also have a constant velocity model due to the free rotations of the mouse. In the complement subspace dynamics is tightly constrained reflecting a strong prior knowledge. The uncertainty of the measures has been set to s_D=2 pixels and the estimated deformation parameter in the Sobolev space to b=2.5 The Wavelet function has been Daubechies D_{12}.

In Figure 4 some results of the tracking process are shown. It is seen how the tracking algorithm follows with precision the mouse on its movement in the cell. Notice by seeing images 4 and 9 of the sequence that the mouse movement has a strong elongation that can be determined through the model.

Figure 4 about here

8.2 Contour tracking with the Condensation filter

When there is substantial clutter the gaussian approximation for the probability distribution of the measurement process is not valid. In complex or cluttered environments there are several observations that can be matched to the contour generating multimodal distributions. To track shape over different frames the Condensation filter [17], [20], [21] has been employed. It uses a set of samples to approximate the probability density function of the tracking process.

A generalized observation model in this case can be set as follows. In one dimension observations reduce to a set of scalar positions $\boldsymbol{Z}=(d_1, d_{2,\ldots,} d_m)$ and the observation density has the form $P(\boldsymbol{Z} \mid x)$ where x is a scalar position. Then a density function can be defined as [20]:

$$p(\boldsymbol{Z} \mid x) \propto 1+\frac{1}{\sqrt{2\pi}\,\sigma\,\alpha}\sum_m e^{-\frac{(d_m-x)^2}{2\sigma^2}}, \tag{8.6}$$

where σ represents the uncertainty in position of the scalar positions d_i and α balances the distribution in case that no one of the d_i in vector $\boldsymbol{Z}$ corresponds to x. In two dimensions the probability distribution is constructed as the product of one-dimensional densities, evaluated independently along curve normals.

The Condensation filter is based on approximating the desired distribution at time t by a set Q_t of samples $\hat{\boldsymbol{q}}_t^{(i)}$ weighted with discrete probabilities $p_{t-1}^{(i)}$. Therefore:

$$Q_{t-1}=\{\hat{\boldsymbol{q}}_{t-1}^{(i)}, p_{t-1}^{(i)}, i=1...N_Q\}, \quad \hat{\boldsymbol{q}}_{t-1}^{(i)}=(\hat{\boldsymbol{x}}_{t-1}^{(i)}, \hat{\boldsymbol{x}}_{t-2}^{(i)}), \tag{8.7}$$

then this sample set evolves in time using the evolution equations of the Condensation filter. These equations are applied in two steps:

1. - Prediction

Approximate the prior distribution generating new elements $\hat{\boldsymbol{q}}'^{(i)}_{t-1}=(\hat{\boldsymbol{x}}'^{(i)}_{t-1}, \hat{\boldsymbol{x}}'^{(i)}_{t-2})$, i=1..N_Q sampling with replacement from Q_{t-1}.

Evaluate a shape space prediction as:

$$\hat{\boldsymbol{x}}_t^{-(i)} - \bar{\boldsymbol{x}} = \boldsymbol{A_1}(\hat{\boldsymbol{x}}'^{(i)}_{t-1} - \bar{\boldsymbol{x}}) + \boldsymbol{A_2}(\hat{\boldsymbol{x}}'^{(i)}_{t-2} - \bar{\boldsymbol{x}}) + \boldsymbol{S}_x^{-1/2}\boldsymbol{n}_t^{(i)}, \qquad \hat{\boldsymbol{x}}_{t-1}^{-(i)} = \hat{\boldsymbol{x}}'^{(i)}_{t-1}, \tag{8.8}$$

where $\boldsymbol{n}_t^{(i)}$ is a sample from a zero mean identity covariance normal distribution.

2.- Measure

For every sample evaluate the adjustment probability:

$$p_t^{(i)} = p(\boldsymbol{Z}_t \mid \boldsymbol{x}_t = \hat{\boldsymbol{x}}_t^{-(i)}), \tag{8.9}$$

and normalize so that: $\sum_i p_k^{(i)} = 1$.

In Figure 4 we show an example of tracking with the Condensation filter. The problem to be solved is to follow the outline of a part of a robotic arm in a laboratory setting. In this case the Kalman filter is not appropriate since the environment is complex. There are several sources that may distract the tracker due to the borders found intro the arm and the borders in the background. Change of position and deformation of the arm has two principal components: translation and affine change. We expect the robotic arm to move freely across the image and to have moderate affine deformations. The dynamic model used is the partitioned harmonic motion between subspaces. The parameters have been:

Table 2 about here

The election of the parameters shows that no oscillatory movement is expected. Translational movement is defined with the constant velocity model allowing a free movement through the image and a moderate velocity in the affine subspace is supposed where mean square displacement is set to 25 pixels.

The uncertainty of the measures has been set to s_D=2 pixels and the deformation parameter in the Sobolev space has been estimated to b=1.7. The wavelet function has been Daubechies D_{12}.

In Figure 5 some results of the tracking process are shown. In this case, best 10 members of a population of 100 in set Q are superimposed in the image. It can be seen how the tracking algorithm follows with precision the arm despite its motion and the movement of the camera. Notice by seeing images 1 and 9 of the sequence that the mouse movement has a strong affine component that can be determined through the model.

Figure 5 about here

9 Conclusions

A new model for contour deformations using wavelets has been proposed. It relates contour deformations to Sobolev smoothness spaces. This allows different degrees of smoothness to be enforced without altering the balance of uncertainty between prior deformation model and data extracted from the image. The deformation framework is expressed in terms of linear shape space models combining deformations from the smoothness model with geometric deformations. This deformation model is extended to a dynamic model that can be used to solve the tracking problem. Experimental results are shown for both the fitting and tracking problem with the Kalman and Condensation filter in real images and results are discussed. They show how this approach increases the robustness of the solutions and successfully follow the shape of the objects in the images.

10. References

[1] T. McInerney, D. Terzopoulos, Deformable models in medical images analysis: a survey, Medical Image Analysis 1(2) (1996) 91-108.

[2] M. Kass, A. Witkin, D. Terzopoulos, Snakes: active contour models, Int. Journal of Comp.Vision, 1 (1988), 321-331.

[3] S. Menet, P. Saint Marc, G. Medioni, B-snakes: Implementations and applications to stereo. Image Understanding Workshop, 1990, pp. 720-726.

[4] L. H. Staib, J.S. Duncan. Boundary finding with parametrically deformable models, IEEE Transactions On Pattern Analysis and Machine Intelligence, 14 (11) (1992) 1061-1075.

[5] D. Reynard, A. Wildenberg, A. Blake. Learning dynamics of complex motions from image sequences. Proc. 4th European conference on Computer Vision, 1996, pp. 357-368.

[6] N. Ayache, I. Cohen, I. Herlin, Medical image tracking. In A. Blake and A. Yuille, editors, Active Vision, pp. 285-302. MIT Press, Cambridge, MA, 1992.

[7] G. Sullivan, Visual interpretation of known objects in constrained scenes, Phil. Trans. Roy. Soc. London B, 337 (1992) 109-118.

[8] J. Luettin, N. Thacker, S. Beet, Visual speech recognition using active shape models and hidden markov models. Proc. IEEE ICASSP, 1996, pp. 817-820.

[9] G.C.H. Chuang, C.C.J. Kuo, Wavelet descriptor of planar curves: Theory and Applications. IEEE Trans. on Image Processing, 5(1), (1996) 56-70.

[10] C. Knoll, M. Alcañiz, V. Grau, C. Monserrat, M.C. Juan, Outlining of the prostate using snakes with shape restrictions based on the wavelet transform, Pattern Recognition 32 (1999) 1767-1781.

[11] H. Yoshida, S. Katsuragawa, Y. Amit, K. Doi, Wavelet Snake for Classification of Nodules and False Positives in Digital Chest Radiographs. Proc IEEE Engineering in Medicine and Biology Society, 1997, pp. 509-512.

[12] H. Choi, R. Baraniuk, Wavelet-domain statistical models and Besov spaces. Proc. of SPIE Technical conference on Wavelet Applications in Signal Processing VII, 1999, pp. 489-501.

[13] S. G. Mallat, A theory for multiresolution signal decomposition: The wavelet representation. IEEE Transactions on Pattern Analysis and Machine Intelligence 11(7) (1989) 674-693.

[14] B. Jawerth, W. Sweldens, An overview of wavelet based multiresolution analyses, SIAM Rev. 36(3), (1994), 377-412.

[15] P. Wojtaszczyk. A Mathematical Introduction to Wavelets. London Mathematical Society Student Texts 37, Cambridge University Press, Cambridge, 1997.

[16] A. De Vore, Non linear approximation, Acta Numerica (1998) 51-150.

[17] A. Blake, M. Isard, Active Contours, Springer-Verlag, London, 1998.

[18] A. Blake, R. Curwen, A. Zisserman, A framework for spatio-temporal control in the tracking of visual contours, International Journal of Computer Vision, 11(2) (1993) 127-145.

[19] P. S. Maybeck, The Kalman Filter: An Introduction to Concepts , in Cox and Wilfong, eds. Autonomous Robot Vehicles. Springer Verlag, Berlin, 1990, pp. 193-204.

[20] M. Isard. Visual motion analysis by probabilistic propagation of conditional density. PhD thesis, Department of Engineering Science, University of Oxford, 1998.

[21] A. Blake, M. Isard, J. MacCormick, Statistical models of visual shape and motion in A. Doucet N. de Freitas, N. Gordon eds. Sequential Montecarlo Methods in Practice, Springer-Verlag, New York, 2001, pp. 339-358.

About the Author – FERNANDO PÉREZ NAVA graduated in 1989 from La Laguna University in Mathematics. From 1989 to 1992 he worked in Galileo Ingeniería y Servicios where he participated in several European projects related to Pattern Recognition. In 1992 he joined the Departamento de Estadística, Investigación Operativa y Computación at La Laguna University. He received the doctorate degree in 2001 from La Laguna University. His research interests include Pattern Recognition, Signal Processing and Computer Vision. Currently he is professor of Computer Science at the University of La Laguna.

About the Author – ANTONIO FALCÓN MARTEL graduated in 1981 from Las Palmas Polytechnic University in Electrical Engineering. He received the doctorate degree in 1983 from the Canarias Polytechnic University. Until 1987, he was a member of Electronic Department of Industrial Engineering School of Las Palmas. Between 1987 and 1992 he worked as post-doctoral researcher at the Cybernetic and Systems Laboratory of Las Palmas de G.C University. His research interests include Computer Vision Systems and Scene Analysis. Currently he is professor of Computer Science and Engineering at the Computer Science and Systems Department and senior research of Intelligent Systems Research Institute at the University of Las Palmas.

Wavelet Modeling of Contour Deformations in Sobolev Spaces for fitting and tracking applications

Fernando Pérez Nava[a], Antonio Falcón Martel[b]

[a]Dep. de Estadística, Investigación Operativa y Computación. Universidad de La Laguna. Tenerife. Spain
[b]Dep. de Informática y Sistemas, Universidad de Las Palmas de Gran Canaria. Gran Canaria. Spain

Summary. This paper proposes a new model for contour deformations using wavelets. Contour deformations can then be used to characterize objects that possess shape-varying capability, so they can be employed to represent non-rigid objects. This new model extends to contours the relationship between the wavelet decomposition of real functions and Sobolev spaces. As Sobolev spaces are smoothness spaces, this allows controlling the smoothness of the contour deformation extending previous contour wavelet representations.

A deformable model is usually described by a vector of parameters that span a multidimensional space. Usually deformations are confined in a region of the whole space and prior information about preferred deformations of the model can be obtained. Restricting contour deformations with prior models simplifies and increases the robustness of the solutions to some problems like fitting and tracking. The importance of smoothness is that it provides a natural prior in absence of other type of information since many object deformations have a determined degree of smoothness.

We use the wavelet deformation model to solve the fitting and tracking problem. These problems can be set in bayesian probabilistic terms. The bayesian framework handles uncertainty in a natural manner and forces to make explicit all the modeling assumptions. We introduce a probabilistic model for the wavelet deformation of the contour that induces a prior distribution for contour deformation. We also show how this prior can be stated in terms of a gaussian distribution with an exponential decay of variances. This allows solving the fitting problem of the deformable contour to an image by evaluating the maximum of the a posteriori distribution.

Prior models are of importance not only in the fitting problem. They are also of interest in the tracking problem since they restrict the region in the multidimensional space for the parameters of the deformable contour in each image of a sequence. The prior model presented for the fitting problem is then extended to deal with the problem of tracking the contour over a sequence of images. This prior model is set in probabilistic terms using a second order autoregressive stochastic dynamic model for contour evolution in time.

When images are simple and noise free the adjustment density of the contour to the image can be expressed through a normal distribution. This poses the tracking problem into the Kalman filter framework that computes the evolution of the parameter that defines the probabilistic densities over time. However, the gaussian approximation is not valid in images of high complexity and clutter. In that case, other approaches such as the Condensation filter can be used to solve the tracking problem on more difficult domains.

To handle both kinds of situations we express the time evolution equations for these filters, we apply the theoretical models to several real image problems with different degrees of complexity showing the results both the Kalman, and Condensation filters.

Figure captions

Figure 1 Multiresolution decomposition of shape

Figure 2 Realizations of the probabilistic model. Smoothness parameter values are b=0 (left) and b=1.6 (right)

Figure 3 The fitting problem with different smoothing priors. Values for b are b=0 (left) and b=2.5 (right)

Figure 4 Tracking with the Kalman Filter. Images are numbered 1-9 left to right and top to bottom

Figure 5 Tracking with the Condensation filter. Images are numbered 1-9 top to bottom and left to right

Figure 1

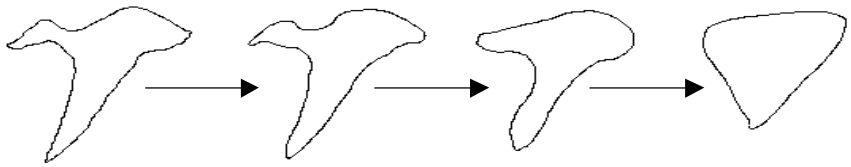

Figure 2

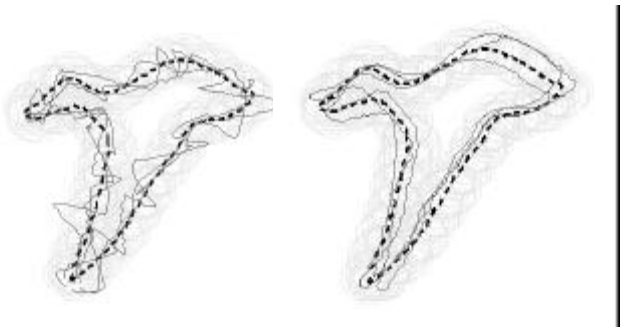

Figure 3

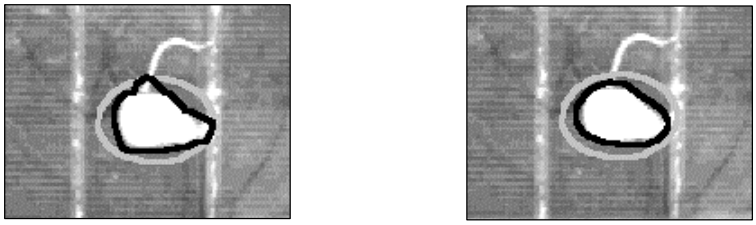

Figure 4

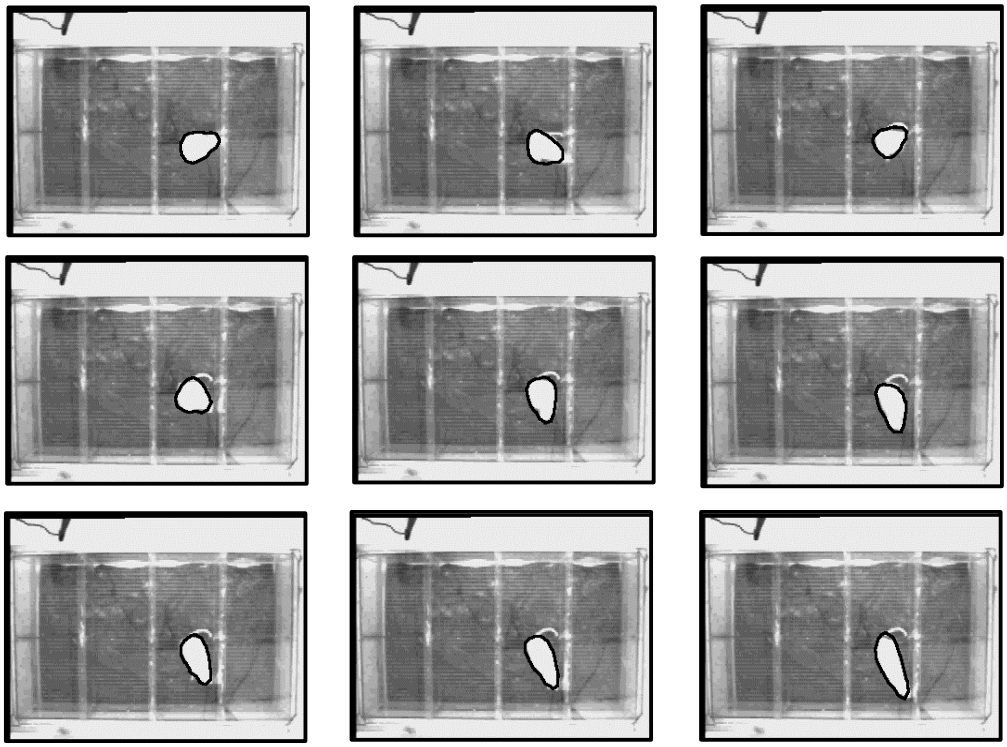

Figure 5

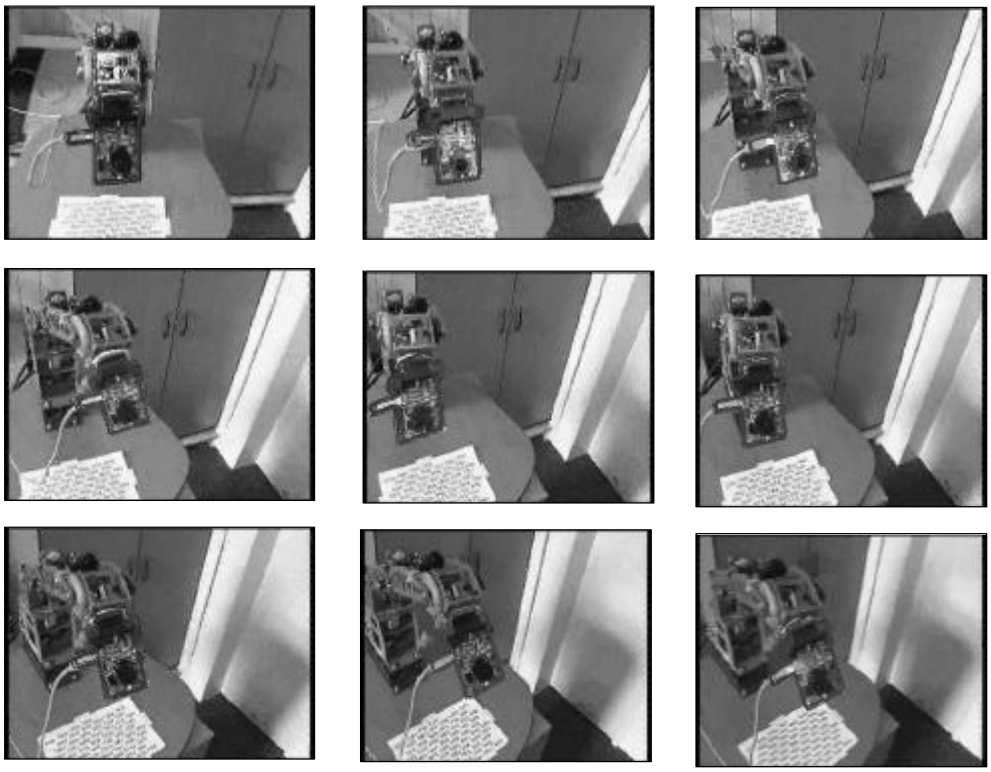

Table captions

Table 1 Dynamical parameters on each subspace for the mouse example

Table 2 Dynamical parameters on each subspace for the robotic arm example

Table 1

Translation	d= 0	f=0	g=12
Key Frame	d= 0	f=0	g=15
Complement	d=10	f=0	$\bar{r}$ =2

Table 2

Translation	d= 0	f=0	g=20
Affine	d=5	f=0	$\bar{r}$ =5